Physics Letters B 827 (2022) 136957

Contents lists available at ScienceDirect

Physics Letters B

www.elsevier.com/locate/physletb

Unveiling the two-proton halo character of ^{17}Ne: Exclusive measurement of quasi-free proton-knockout reactions

C. Lehr [a], F. Wamers [a,b], F. Aksouh [a,b,1], Yu. Aksyutina [b], H. Álvarez-Pol [c], L. Atar [a,b], T. Aumann [a,b,d,*], S. Beceiro-Novo [c,2], C.A. Bertulani [e], K. Boretzky [b], M.J.G. Borge [f], C. Caesar [a,b], M. Chartier [g], A. Chatillon [b], L.V. Chulkov [b,h], D. Cortina-Gil [c], P. Díaz Fernández [c,i], H. Emling [b], O. Ershova [b,j], L.M. Fraile [k], H.O.U. Fynbo [l], D. Galaviz [f], H. Geissel [b], M. Heil [b], M. Heine [a], D.H.H. Hoffmann [a], M. Holl [a,b,i], H.T. Johansson [i], B. Jonson [i], C. Karagiannis [b], O.A. Kiselev [b], J.V. Kratz [m], R. Kulessa [n,o], N. Kurz [b], C. Langer [b,j,3], M. Lantz [i,4], T. Le Bleis [b,p], R. Lemmon [q], Yu.A. Litvinov [b], B. Löher [b,a], K. Mahata [b,r], J. Marganiec-Galązka [a,5], C. Müntz [j], T. Nilsson [i], C. Nociforo [b], W. Ott [b,6], V. Panin [b,a], S. Paschalis [b,g,7], A. Perea [f], R. Plag [b,j], R. Reifarth [j,b], A. Richter [a], K. Riisager [l], C. Rodriguez-Tajes [c], D. Rossi [a,b,m], D. Savran [b], H. Scheit [a], G. Schrieder [a], P. Schrock [a], H. Simon [b], J. Stroth [j,b], K. Sümmerer [b], O. Tengblad [f], H. Weick [b], C. Wimmer [j,b]

[a] Technische Universität Darmstadt, Department of Physics, D–64289 Darmstadt, Germany
[b] GSI Helmholtzzentrum für Schwerionenforschung GmbH, D–64291 Darmstadt, Germany
[c] Instituto Galego de Física de Altas Enerxias, Universidade de Santiago de Compostela, ES–15782 Santiago de Compostela, Spain
[d] Helmholtz Research Academy Hesse for FAIR, D–64289 Darmstadt, Germany
[e] Texas A&M University-Commerce, Commerce, USA
[f] Instituto de Estructura de la Materia, CSIC, ES–28006 Madrid, Spain
[g] Department of Physics, University of Liverpool, Liverpool L69 3BX, United Kingdom
[h] NRC Kurchatov Institute, RU–123182 Moscow, Russia
[i] Department of Physics, Chalmers Tekniska Högskola, SE–41296 Göteborg, Sweden
[j] Goethe Universität Frankfurt, Department of Physics, D–60438 Frankfurt am Main, Germany
[k] Grupo de Física Nuclear & IPARCOS, Universidad Complutense de Madrid, CEI Moncloa, ES–28040 Madrid, Spain
[l] Department of Physics and Astronomy, University of Aarhus, DK–8000 Aarhus, Denmark
[m] Institut für Kernchemie, Johannes Gutenberg-Universität Mainz, D–55122 Mainz, Germany
[n] Instytut Fizyki, Uniwersytet Jagelloński, PL–30-059 Krakóv, Poland
[o] Instytut Fizyki im. Mariana Smoluchowskiego UJ, ul. Prof. St. Łojasiewicza 11, PL–30-348 Krakóv, Poland
[p] Physik-Department E12, Technische Universität München, D–85748 Garching, Germany
[q] Nuclear Physics Group, STFC Daresbury Lab, Warrington WA4 4AD, Cheshire, United Kingdom
[r] Nuclear Physics Division, Bhabha Atomic Research Centre, Trombay, Mumbai-400 085, India

ARTICLE INFO

Article history:
Received 24 August 2021
Received in revised form 1 February 2022
Accepted 7 February 2022
Available online 15 February 2022
Editor: B. Blank

ABSTRACT

The proton drip-line nucleus ^{17}Ne is investigated experimentally in order to determine its two-proton halo character. A fully exclusive measurement of the $^{17}\mathrm{Ne}(p,2p)^{16}\mathrm{F}^{*} \rightarrow ^{15}\mathrm{O}+p$ quasi-free one-proton knockout reaction has been performed at GSI at around 500 MeV/nucleon beam energy. All particles resulting from the scattering process have been detected. The relevant reconstructed quantities are the angles of the two protons scattered in quasi-elastic kinematics, the decay of ^{16}F into ^{15}O (including γ decays from excited states) and a proton, as well as the $^{15}\mathrm{O}+p$ relative-energy spectrum and the ^{16}F

* Corresponding author at: Technische Universität Darmstadt, Department of Physics, D–64289 Darmstadt, Germany.
E-mail address: thomas.aumann@tu-darmstadt.de (T. Aumann).
[1] *Present address:* Department of Physics and Astronomy, College of Science, King Saud University, P.O. Box 2455, 11451 Riyadh, KSA.
[2] *Present address:* NSCL, Michigan State University, East Lansing, Michigan 48824, USA.
[3] *Present address:* FH Aachen University of Applied Science, D–52066 Aachen, Germany.
[4] *Present address:* Department of Physics and Astronomy, Uppsala University, SE–751 20 Uppsala, Sweden.
[5] *Present address:* National Centre for Nuclear Research, Radioisotope Centre POLATOM, 05-400 Otwock, Poland.
[6] Deceased.
[7] *Present address:* Department of Physics, University of York, York, YO10 5DD, UK.

https://doi.org/10.1016/j.physletb.2022.136957

momentum distributions. The latter two quantities allow an independent and consistent determination of the fractions of $l = 0$ and $l = 2$ motion of the valence protons in ^{17}Ne. With a resulting relatively small $l = 0$ component of only around 35(3)%, it is concluded that ^{17}Ne exhibits a rather modest halo character only. The quantitative agreement of the two values deduced from the energy spectrum and the momentum distributions supports the theoretical treatment of the calculation of momentum distributions after quasi-free knockout reactions at high energies by taking into account distortions based on the Glauber theory. Moreover, the experimental data allow the separation of valence-proton knockout and knockout from the ^{15}O core. The latter process contributes with 11.8(3.1) mb around 40% to the total proton-knockout cross section of 30.3(2.3) mb, which explains previously reported contradicting conclusions derived from inclusive cross sections.

1. Introduction

Atomic nuclei at the limits of nuclear binding, located close to the neutron and proton drip lines, exhibit unusual and often unexpected properties when compared to expectations from theoretical models, which describe known properties of ordinary stable or very long-lived nuclei well. Because of the closeness of the continuum, such nuclei are called 'open quantum systems', often dominated by correlations [1]. The experimental study of properties of drip-line nuclei is thus key for developing and testing modern nuclear theory and the interactions used. The knowledge of properties of exotic nuclei, either reliably theoretically predicted or directly measured, is also a basis for the understanding of nucleosynthesis processes in astrophysics, such as the rapid proton- and neutron-capture processes.

Particular attention in this direction was dedicated to halo nuclei since their experimental discovery at the Berkeley BEVALAC by Tanihata et al. [2,3] and the following interpretation and name coining nuclear 'halo' by Hansen and Jonson [4]. Halo nuclei exhibit a matter-density distribution with a pronounced, far-extending, low-density tail (halo), which is caused by the wavefunction of the last weakly-bound valence nucleons, which reaches far into the classical forbidden region. This generates an almost pure neutron or proton low-density environment at the surface of the nucleus. On the neutron drip-line, several such nuclei have been studied in great detail, thanks to the tremendous progress in rare-isotope beam accelerator facilities and experimental instrumentation. A prime example is ^{11}Li with two loosely-bound neutrons forming the halo, where the two neutrons are strongly correlated in a mixed ground-state wavefunction comprising components with angular momenta $l = 0$ and $l = 1$ [5,6]. A sizable low-angular-momentum component is essential for the formation of a halo-like structure.

On the much-less studied proton drip-line side, ^{17}Ne is the most promising candidate for such a structure. In a three-body model, ^{17}Ne can be described as a well bound ^{15}O core plus two protons loosely bound with a two-proton separation energy of only $S_{2p} = 933.1(6)$ keV [7]. According to the standard nuclear shell model, the oxygen core has a closed proton shell, with the next available states in the *sd* shell. For the given separation energy of the ^{17}Ne case, the *rms* radii of the $l = 0$ and $l = 2$ valence-nucleon wavefunctions are 4.3 fm and 3.5 fm, respectively, which compares to a *rms* radius of 2.6 fm for the ^{15}O core. This suggests the possibility of halo formation with the two protons in $l = 0$ motion [8]. Moreover, like ^{11}Li, with both sub-systems (^{16}F and $p - p$) being unbound, ^{17}Ne is a *Borromean* nucleus. Albeit numerous experimental efforts, a firm conclusion on the structure of ^{17}Ne has not yet been reached. In this Letter, we present experimental results from an exclusive measurement of the $(p, 2p)$ proton knockout reaction. The fraction of the s^2 and d^2 components in the valence-nucleon motion have been determined by two independently measured quantities, providing a clear answer to this long-standing discussion. With a resulting s^2 to d^2 ratio of around $\frac{1}{3}$ to $\frac{2}{3}$, it is concluded that ^{17}Ne exhibits only a rather moderate halo character.

2. Summary of the ^{17}Ne puzzle

Evidence for a proton halo in ^{17}Ne, *i.e.*, a dominance of the $(s_{1/2})^2$ configuration in the valence-proton wavefunction was claimed from measurements of total interaction cross sections for $A = 17$ high-energy beams [9]. However, calculations of the interaction cross section based on Hartree-Fock-type wave functions and the Glauber model result in the opposite conclusion with a dominance of the $(1d_{5/2})^2$ configuration [10]. An (l=0)-dominated two-proton halo structure of ^{17}Ne was also inferred from an analysis of the ^{15}O momentum distribution and cross section for the inclusive $2p$-removal reaction at 66 MeV/nucleon [11,12], while a shell-model interpretation of the magnetic-moment measurement [13] arrives at the opposite conclusion. Furthermore, the measured charge radii for ^{17,18,19}Ne of 3.04(2), 2.97(2), and 3.01(1) fm [14] do not support a pronounced halo for ^{17}Ne. An analysis in the theoretical framework of fermionic molecular dynamics (FMD) relates the charge radius to the s^2 occupation by tuning the interaction resulting in a possible range of 38-46% s^2 occupation assuming that only the two valence nucleons contribute to the change of the charge radius. Results from theoretical predictions span the full range from s^2 dominance to d^2 dominance. A summary of obtained experimental and theoretical estimates is given in the Supplemental Material.

Clearly, a more exclusive measurement of observables with high sensitivity and selectivity to distinguish the $l = 0$ and $l = 2$ contributions for the two weakly-bound valence protons is mandatory to conclude on the halo character of ^{17}Ne. The quasi-free proton-knockout reaction described in this Letter provides this sensitivity. The populated resonances with known structure are identified via invariant-mass spectroscopy of the residual fragment. The shape of the measured momentum distribution is sensitive to the slope of the nuclear density distribution at the surface, which is dominated by the exponential decay of the least-bound nucleon's wavefunction, which strongly depends on the angular momentum due to the angular-momentum barrier. The different shapes of the *s* and *d* density distributions at the surface result in different shapes of the measured momentum distributions. The extraction of the relative weights of s^2 and d^2 components is thus rather direct and less model dependent.

3. Experiment

The primary ^{20}Ne beam was extracted from the GSI synchrotron SIS18 with an energy of 630 MeV/nucleon and directed to the production target at the fragment separator FRS. The secondary ^{17}Ne beam entered the experimental area Cave C at GSI with an average energy of 498 MeV/nucleon in the middle of the CH_2 target

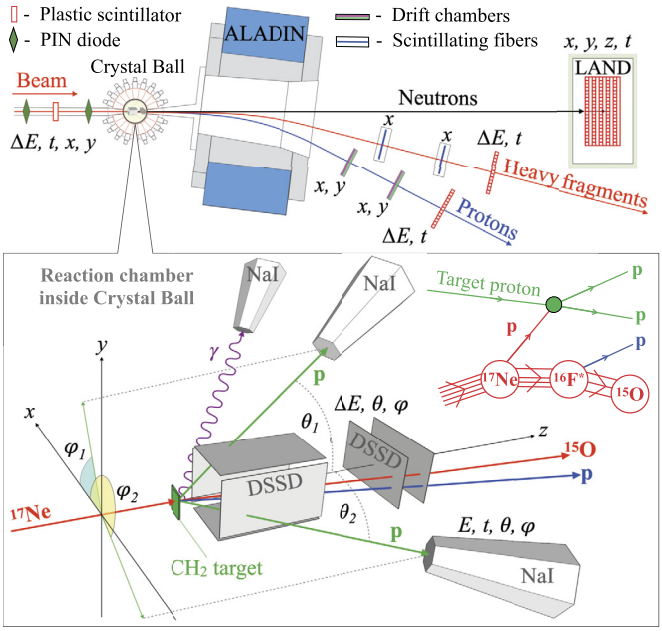

Fig. 1. Schematic drawing of the experimental setup (not to scale). The upper part indicates the detection systems and measured quantities to track and identify projectiles and forward-emitted reaction products. The lower frame provides a more detailed view of the detection systems around the target and the reaction studied. Photons are detected with NaI crystals, protons with double-sided Si-strip detectors (DSSD) and NaI crystals.

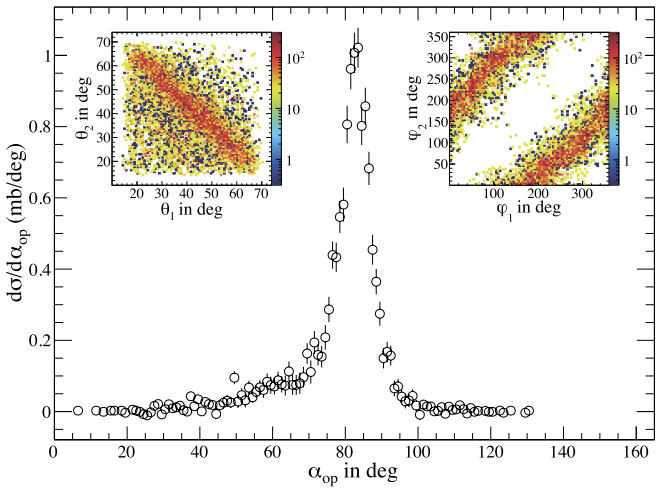

Fig. 2. Angular correlations of the two scattered protons in the $(p, 2p)$ knockout reaction. The insets display the correlations between the polar (left) and azimuthal (right) angles. The main figure shows the distribution as function of the projected opening angle $\alpha_{op} = \theta_1 + \theta_2$ of the two protons.

with a thickness of 213 mg/cm^2. The secondary beam on target contained $>$ 90% ^{17}Ne with an average intensity of identified and tracked ^{17}Ne ions of around 3×10^3/s during the beam-on phase. The beam energy of 500 MeV/nucleon was chosen to minimize secondary reactions of protons in the nuclear medium after the primary pp scattering process. The energy of the outgoing protons is on average 250 MeV at scattering angles of around 45°, for which the nucleon-nucleon (NN) cross section is minimal. The experimental setup is schematically shown in Fig. 1, and is identical to the one described in Refs. [15,16,18]. The quasi-free one-proton knockout reaction $^{17}\mathrm{Ne}(p, 2p)^{16}\mathrm{F}^* \rightarrow ^{15}\mathrm{O}{+}p$ has been analyzed. In order to determine reactions induced by the carbon content in the CH_2 target and in other materials outside the target, additional measurements have been performed with C target (370 mg/cm^2) as well as without target. The experimental method of quasi-free scattering in inverse kinematics has been established before using the $^{12}\mathrm{C}(p, 2p)$ reaction [16]. Identified ^{17}Ne incoming ions are tracked with position-sensitive silicon PIN diodes towards the target. After the reaction target, outgoing fragments are deflected in the large-gap dipole magnet ALADIN and identified. Their angles, velocity, and magnetic rigidity are determined by double-sided silicon micro-strip detectors (DSSD), scintillating fibre detectors, and a time-of-flight (ToF) wall. For the reaction channel of interest, identified ^{15}O fragments have been selected.

The $(p, 2p)$ reaction channel is further characterized by the measurement of the angular distribution of the two scattered protons (including the target proton), and the forward emitted proton from the decay of unbound ^{16}F states populated after proton knockout. A more detailed description of the quasi-free knockout reaction in inverse kinematics and summary of experiments using this method so far can be found in Ref. [17]. The scattered protons are detected by a box of four DSSDs covering an angular range of 15° to 72°, and the Crystal Ball (CB) consisting of 162 individual NaI crystals surrounding the target (see lower part of Fig. 1). The resulting angular distributions of scattered protons are displayed in Fig. 2. The angles are defined in the laboratory system with the z-axis pointing along the beam-particles trajectory (see lower part of Fig. 1). They exhibit a back-to-back scattering with an opening angle peaking at around 84° as expected for quasi-free NN scattering. Deviations from elastic pp scattering like the width of the distributions and the slightly reduced average opening angle have their origin in the internal motion of the proton in ^{17}Ne and its binding energy relative to that of the final state.

Protons originating from the decay in flight of ^{16}F are emitted in the laboratory frame at forward angles and tracked through the dipole magnet by two DSSDs located before the magnet, and drift chambers plus a ToF wall after the magnet. γ decays from excited states are detected by the CB spectrometer and calorimeter. The excitation-energy spectrum and momentum distributions of ^{16}F produced in the proton knockout reaction are calculated from the measured momenta of the decay products p and ^{15}O by applying the invariant-mass method. The resulting resolutions are around 0.1 MeV at 1 MeV relative energy and 26 MeV/c for the transverse momentum (see Supplemental Material for more details).

4. Results

The resulting differential cross section $d\sigma/dE_{\mathrm{fp}}$ as a function of the relative energy E_{fp} between the ^{15}O fragment and the decay proton for the reaction $^{17}\mathrm{Ne}(p, 2p)^{16}\mathrm{F}^* \rightarrow ^{15}\mathrm{O}{+}p$ is shown in Fig. 3, where contributions of around 10% associated with additional γ-decays related to knockout of core protons, were subtracted. The measured γ-spectrum is shown in Fig. 7 of the Supplemental Material, where also details on the subtraction procedure are given. The spectrum exhibits two clear structures. The peak structure at higher energies reflects the population of high-lying excited states in ^{16}F after knockout of a proton from the ^{15}O core in ^{17}Ne (see level scheme given in Fig. 3). Together with the decays accompanied by additional γ decays, the core knockout reaction contributes with 11.8(3.1) mb around 40% to the total one-proton knockout cross section $\sigma_{(p,2p)} = 30.3(2.3)$ mb.

The low-lying peak results from the population of single-particle states of ^{16}F, which are not resolved in our measurement. The black solid line shows a fit to the data consisting of a sum of Breit-Wigner curves with known energies and widths of the resonances adopted from the literature [19], taking into account the different penetrabilities for the $l = 0$ and $l = 2$ states (details are provided in the Supplemental Material). After taking into account the experimental response, the visible width and shape

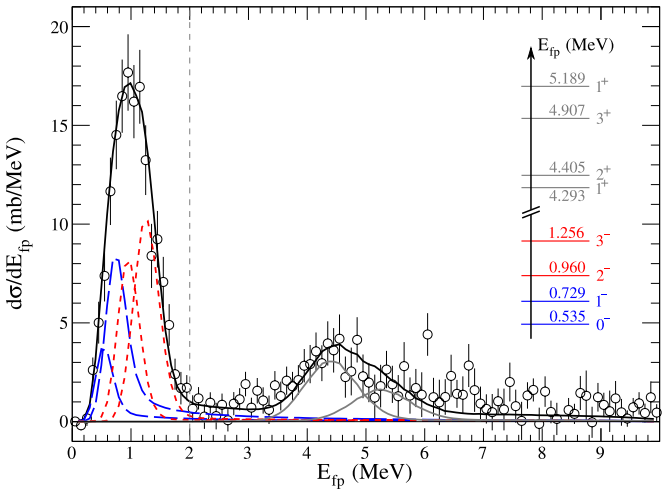

Fig. 3. Differential cross section $d\sigma/dE_{\rm fp}$ as function of the relative energy $E_{\rm fp}$ between the ^{15}O fragment and the decay proton for the reaction ^{17}Ne$(p,2p)^{16}$F$^{*}\rightarrow^{15}$O$+p$. Contributions involving γ-decays have been subtracted. The prominent peak below 2 MeV results from four low-lying resonances in ^{16}F populated after knockout of a valence proton from ^{17}Ne, while the cumulation of events between 3 and 6 MeV corresponds to knockout of a proton from the ^{15}O core. The inset shows the populated states with their energy and quantum numbers.

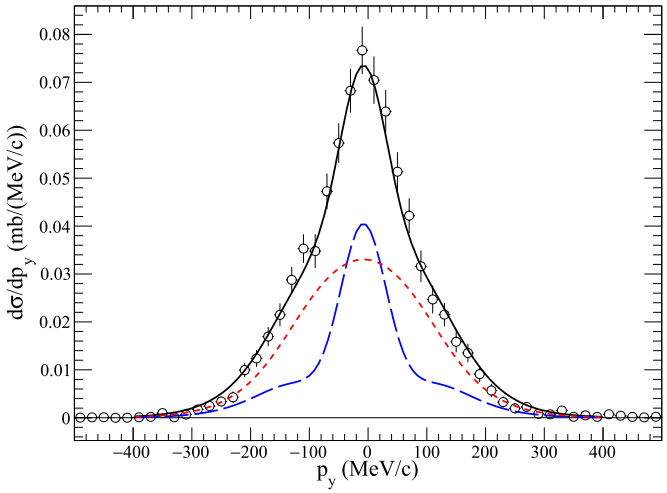

Fig. 4. Momentum distribution $d\sigma/dp_y$ of ^{16}F projected onto the cartesian coordinate y perpendicular to the beam for the reaction ^{17}Ne$(p,2p)^{16}$F$^{*}\rightarrow^{15}$O$+p$ with the condition $E_{\rm fp}<2$ MeV. The solid curve represents the theoretical result after adjusting the $l=0$ (long-dashed) and $l=2$ (short-dashed) contributions to the experimental data (symbols).

of the resonances are dominated by the resolution resulting in a Gaussian-like shape in the peak region. Therefore, the description of the spectrum is rather insensitive to the details of the line shape and additional uncertainties which could arise due to this are negligible.

The two low-lying 0^- and 1^- states (see level scheme shown in Fig. 3) are s-wave resonances populated after the knockout of a valence proton from the s^2 configuration, while the two higher lying 2^- and 3^- states are the d-resonances in ^{16}F populated after knockout from the d^2 configuration. The properties of the resonances have been precisely determined by different experiments showing their rather pure $s_{1/2}$ and $d_{5/2}$ single-particle structure [20].

The low-energy part of the spectrum below 2 MeV corresponds thus to the valence-proton or 'halo' knockout. The fit results in a cross section of 18.5(2.1) mb for the halo knockout with a relative contribution for the population of the s-states of 42(5)% The high-energy positive-parity states of the spectrum above 2 MeV are populated in core knockout reactions. The grey curves indicate the fit result, where the two groups of non-resolved resonances are approximated by two Breit-Wigner curves.

The experimental cross sections are compared to theoretical $(p,2p)$ quasi-free-scattering cross sections computed using the Glauber theory [21]. Inputs to the calculations are the ^{15}O core density distribution, single-particle wave functions for the valence protons, and the free NN cross sections. A Hartree-Fock density is used for the core with a radius $r_{rms}=2.64$ fm. The single-particle wave functions were obtained by solving the Schrödinger equation for a Woods-Saxon mean-field potential with radius parameter $r_0=1.2$ fm and diffuseness $a=0.7$ fm. Cross sections were computed individually for the angular momenta $l=0$ and $l=2$ and effective binding energies according to the resonances populated. The obtained single-particle cross sections σ_{sp} for the s and d states are 11.65 mb and 9.16 mb, respectively. The cross section for $l=0$ is somewhat larger due to the surface-dominated reaction probability and the long halo-like tail of the s wavefunction. This results in spectroscopic factors of $C^2S=0.67(11)$ for the s^2 configuration and $C^2S=1.17(16)$ for the d^2 configuration, where $C^2S=\sigma_{exp}/\sigma_{sp}$. The given uncertainties in comparing with the Glauber theory do not include theoretical uncertainties. The probability $P(\frac{s^2}{s^2+d^2})$ to find the two valence protons in the s^2 configuration in the ^{17}Ne ground state amounts thus to 36(5)%.

The shape of the momentum distribution $d\sigma/dp$ of the residual fragment after one-nucleon knockout is characteristic for the angular momentum of the knocked-out nucleon. The transverse momentum distribution $d\sigma/dp_y$ of ^{16}F, projected onto the cartesian coordinate y, is shown in Fig. 4. The distribution was reconstructed from the measured momenta of ^{15}O plus the forward-emitted proton from the decay of ^{16}F, with the condition that the relative energy $E_{\rm fp}<2$ MeV, *i.e.*, with a selection on 'halo' knockout. The data clearly indicate a superposition of two shapes. The solid curve represents a fit of the calculated distributions to the data, using the above-described theoretical description, for $l=0$ (long-dashed curve) and $l=2$ (short-dashed curve), obtained from a χ^2 minimization in a simultaneous fit to both transverse momentum distributions (see Fig. 8 in the Supplemental Material). This results in a relative contribution to the cross section of 39(4)% for $l=0$, corresponding to a probability of 34(3)% for the s^2 configuration of the valence protons. This is in perfect agreement with the independent result of 36(5)% derived from the relative-energy spectrum discussed above. The good agreement also corroborates the assumption that the 0^- and 1^- states are pure s states and do not contain a sizable $d_{3/2}$ component. An admixture in the order of 10%, however, cannot be excluded. This would result in an overestimate of the s^2 contribution extracted from the relative-energy spectrum by around 10%, which would still be consistent with the result from the momentum distributions, which is not sensitive to such an admixture and reflects directly the fractions of s^2 and d^2 components.

The dominance of the $l=2$ configuration is further supported by the proton-proton angular correlations in the ^{17}Ne ground state shown in Fig. 5. The $p-p$ relative angle θ_{pp} in the ^{17}Ne frame has been constructed under the assumption that the relative motion of the fragment ^{15}O and the proton p_2 (from the decay of ^{16}F, see inset of Fig. 5) remains undisturbed after sudden knockout of the proton p_1. The angular correlation between the protons in the ^{17}Ne ground state is accordingly reflected by the angle between the momentum of the knocked out proton p_1, given by the ^{16}F recoil with $\mathbf{p}_{p_1}=-\mathbf{p}_{^{16}F}$ (in the rest frame of the projectile), and the ^{15}O$-p_2$ relative momentum $\mathbf{p}_{fp}=\mu(\mathbf{p}_{p_2}/m_p-\mathbf{p}_f/m_f)$, where m_p, m_f, and μ are the masses of proton, ^{15}O, and the reduced mass of the ^{16}F system, respectively.

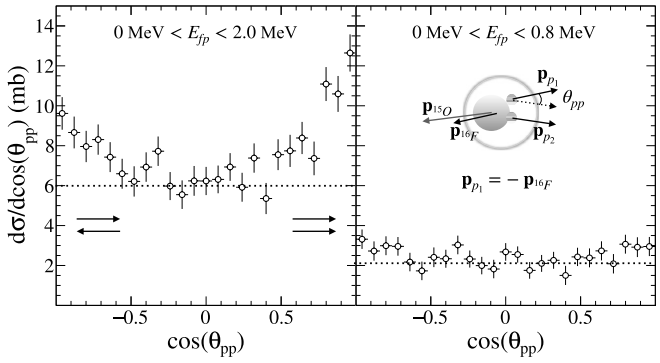

Fig. 5. Proton-proton angular correlation θ_{pp} of the momenta of the two halo protons in ^{17}Ne, represented by the angle between the recoil momentum of ^{16}F and the direction of the ^{15}O$-p$ relative motion (see text). The left frame shows the distribution for halo knockout with population of ^{16}F in the energy region $E_{\rm fp} < 2.0$ MeV with overlapping s and d resonances, while the right frame displays the correlation for $E_{\rm fp} < 0.8$ MeV, where the $l = 0$ configuration dominates. The horizontal dotted lines indicate a symmetric and isotropic distribution to guide the eye.

While a quantitative estimate of the angular correlation in terms of the s^2 and d^2 components needs reliable wavefunctions as an input [5,22,23], we conclude that the angular distribution exhibits a parabolic shape, which is caused by the d-wave contribution with preferred back-to-back or parallel motion (Fig. 5 left frame), while for a pure ($l = 0$)-state, an isotropic distribution is expected [22,23]. This can be seen in the right frame of Fig. 5, where the distribution is shown for the condition $E_{\rm fp} < 0.8$ MeV, for which the $l = 0$ contribution dominates. Only a slight deviation from an isotropic distribution is visible, which is caused by remaining small d admixtures.

5. Conclusion

The structure of the proton-halo candidate ^{17}Ne has been investigated by performing and analyzing an exclusive measurement of the ^{17}Ne$(p, 2p)^{16}$F$^* \rightarrow ^{15}$O$+p$ reaction at high beam energy of around 500 MeV/nucleon. The data allowed for the identification of quasi-free $(p, 2p)$ knockout from the valence states. The analysis of two independent observables, the ^{15}O$-p$ relative-energy spectrum and the ^{16}F momentum distribution, results in a consistent interpretation of the structure of the ^{17}Ne ground-state configuration, where the two valence protons occupy dominantly s^2 and d^2 configurations with a rather small s^2 component of 35(3)%. The dominance of the d^2 contribution suppresses the halo character of ^{17}Ne. The large total spectroscopic factor of $C^2S = 1.8(2)$ indicates no or only minor contributions due to more complex configurations, and supports a description of ^{17}Ne in a ^{15}O$+p+p$ three-body model with an inert ^{15}O core. The large spectroscopic factor for the weakly-bound valence nucleons obtained from this analysis, as compared to stable nuclei, supports a trend as a function of separation energies and/or neutron-proton asymmetry as found in nucleon-removal reactions at intermediate energies (see [24], and [25] for a recent review).

The quantitative agreement of the analysis of two independently measured quantities, the population of final states and the momentum distributions, give confidence on the accuracy of treating the $(p, 2p)$ reaction in the Glauber theory based on eikonal wavefunctions as developed in Ref. [21]. The extraction of the fractions of different configurations from momentum distributions relies on the calculated shape of the distributions, which is affected by distortions due to the reaction mechanism. The perfect agreement of the theoretical shape with the measured distribution in conjunction with a perfect agreement of the extracted s^2 fraction provides a solid basis for the investigation of exotic nuclei using quasi-free scattering at the upcoming radioactive-beam facilities FAIR and FRIB.

The controversial conclusions in the literature on the halo structure of ^{17}Ne can be resolved. We discuss here only the least indirect measurements with sensitivity to the s-wave character of the valence-nucleon wave function, although with a model dependent interpretation: the measurement of the magnetic dipole moment [13] and the inclusive proton-removal reaction [11]. The result presented in this Letter is in agreement with the shell-model interpretation of the magnetic-moment measurement. The different conclusion from the inclusive proton-removal reaction can also be understood at least qualitatively, since core-knockout contributions have been assumed to be small in Ref. [11]. It should be noted, however, that the beam energy used in Ref. [11] was significantly smaller, and that a Be target has been used. The separation of the contributions of the core and valence-nucleon knockout in the exclusive experiment presented here, reveals a significant contribution of around 40% of proton knockout from the core to the total proton-removal cross section.

Declaration of competing interest

The authors declare that they have no known competing financial interests or personal relationships that could have appeared to influence the work reported in this paper.

Acknowledgements

This work is supported by the German Federal Ministry for Education and Research (BMBF) under contract No. 05P15RDFN1, the ExtreMe Matter Institute (EMMI), HIC for FAIR, and the GSI-TU Darmstadt cooperation agreement. Financial support from the Swedish Research Council, from the Russian Foundation for Basic Research (RFBR Grant 12-02-01115-a), and from the Spanish grants from MICINN AEI FPA2017-87568-P, PGC2018-0099746-B-C21, FPA2015-64969-P, PID2019-104390GB-I00, RTI2018-098868-B-100, and Maria de Maeztu Units of excellence MDM-2016-0692 are also acknowledged. One of us (B. J.) is a Helmholtz International Fellow. C.A.B. acknowledges support by the U.S. DOE grant DE-FG02-08ER41533 and the U.S. NSF Grant No. 1415656.

Appendix A. Supplementary material

Supplementary material related to this article can be found online at https://doi.org/10.1016/j.physletb.2022.136957.

References

[1] N. Michel, W. Nazarewicz, M. Płoszajczak, T. Vertse, J. Phys. G, Nucl. Part. Phys. 36 (2008) 013101.
[2] I. Tanihata, H. Hamagaki, O. Hashimoto, S. Nagamiya, Y. Shida, N. Yoshikawa, O. Yamakawa, K. Sugimoto, T. Kobayashi, D. Greiner, N. Takahashi, Y. Nojiri, Phys. Lett. B 160 (1985) 380.
[3] I. Tanihata, H. Hamagaki, O. Hashimoto, Y. Shida, N. Yoshikawa, K. Sugimoto, O. Yamakawa, T. Kobayashi, N. Takahashi, Phys. Rev. Lett. 55 (1985) 2676.
[4] P.G. Hansen, B. Jonson, Europhys. Lett. 4 (1987) 409.
[5] H. Simon, D. Aleksandrov, T. Aumann, L. Axelsson, T. Baumann, M.J.G. Borge, L.V. Chulkov, R. Collatz, J. Cub, W. Dostal, B. Eberlein, T.W. Elze, H. Emling, H. Geissel, A. Grünschloss, M. Hellström, J. Holeczek, R. Holzmann, B. Jonson, J.V. Kratz, G. Kraus, R. Kulessa, Y. Leifels, A. Leistenschneider, T. Leth, I. Mukha, G. Münzenberg, F. Nickel, T. Nilsson, G. Nyman, B. Petersen, M. Pfützner, A. Richter, K. Riisager, C. Scheidenberger, G. Schrieder, W. Schwab, M.H. Smedberg, J. Stroth, A. Surowiec, O. Tengblad, M.V. Zhukov, Phys. Rev. Lett. 83 (1999) 496.
[6] Y. Kubota, A. Corsi, G. Authelet, H. Baba, C. Caesar, D. Calvet, A. Delbart, M. Dozono, J. Feng, F. Flavigny, J.-M. Gheller, J. Gibelin, A. Giganon, A. Gillibert, K. Hasegawa, T. Isobe, Y. Kanaya, S. Kawakami, D. Kim, Y. Kikuchi, Y. Kiyokawa, M. Kobayashi, N. Kobayashi, T. Kobayashi, Y. Kondo, Z. Korkulu, S. Koyama, V. Lapoux, Y. Maeda, F.M. Marqués, T. Motobayashi, T. Miyazaki, T. Nakamura, N. Nakatsuka, Y. Nishio, A. Obertelli, K. Ogata, A. Ohkura, N.A. Orr, S. Ota, H. Otsu,

T. Ozaki, V. Panin, S. Paschalis, E.C. Pollacco, S. Reichert, J.-Y. Roussé, A.T. Saito, S. Sakaguchi, M. Sako, C. Santamaria, M. Sasano, H. Sato, M. Shikata, Y. Shimizu, Y. Shindo, L. Stuhl, T. Sumikama, Y.L. Sun, M. Tabata, Y. Togano, J. Tsubota, Z.H. Yang, J. Yasuda, K. Yoneda, J. Zenihiro, T. Uesaka, Phys. Rev. Lett. 125 (2020) 252501.
[7] M. Wang, W.J. Huang, F.G. Kondev, G. Audi, S. Naimi, Chin. Phys. C 3 (2021) 030003.
[8] M.V. Zhukov, I.J. Thompson, Phys. Rev. C 52 (1995) 3505.
[9] A. Ozawa, T. Kobayashi, H. Sato, D. Hirata, I. Tanihata, O. Yamakawa, K. Omata, K. Sugimoto, D. Olson, W. Christie, H. Wieman, Phys. Lett. B 334 (1994) 18.
[10] H. Kitagawa, N. Tajima, H. Sagawa, Z. Phys. A 358 (1997) 381.
[11] R. Kanungo, M. Chiba, S. Adhikari, D. Fang, N. Iwasa, K. Kimura, K. Maeda, S. Nishimura, Y. Ogawa, T. Ohnishi, Phys. Lett. B 571 (2003) 21.
[12] R. Kanungo, M. Chiba, B. Abu-Ibrahim, S. Adhikari, D.Q. Fang, N. Iwasa, K. Kimura, K. Maeda, S. Nishimura, T. Ohnishi, A. Ozawa, C. Samanta, T. Suda, T. Suzuki, Q. Wang, C. Wu, Y. Yamaguchi, K. Yamada, A. Yoshida, T. Zheng, I. Tanihata, Eur. Phys. J. A 25 (2005) 327.
[13] W. Geithner, B.A. Brown, K.M. Hilligsøe, S. Kappertz, M. Keim, G. Kotrotsios, P. Lievens, K. Marinova, R. Neugart, H. Simon, S. Wilbert, Phys. Rev. C 71 (2005) 064319.
[14] W. Geithner, T. Neff, G. Audi, K. Blaum, P. Delahaye, H. Feldmeier, S. George, C. Guénaut, F. Herfurth, A. Herlert, S. Kappertz, M. Keim, A. Kellerbauer, H.-J. Kluge, M. Kowalska, P. Lievens, D. Lunney, K. Marinova, R. Neugart, L. Schweikhard, S. Wilbert, C. Yazidjian, Phys. Rev. Lett. 101 (2008) 252502.
[15] F. Wamers, J. Marganiec, F. Aksouh, Y. Aksyutina, H. Álvarez-Pol, T. Aumann, S. Beceiro-Novo, K. Boretzky, M.J.G. Borge, M. Chartier, A. Chatillon, L.V. Chulkov, D. Cortina-Gil, H. Emling, O. Ershova, L.M. Fraile, H.O.U. Fynbo, D. Galaviz, H. Geissel, M. Heil, D.H.H. Hoffmann, H.T. Johansson, B. Jonson, C. Karagiannis, O.A. Kiselev, J.V. Kratz, R. Kulessa, N. Kurz, C. Langer, M. Lantz, T. Le Bleis, R. Lemmon, Y.A. Litvinov, K. Mahata, C. Müntz, T. Nilsson, C. Nociforo, G. Nyman, W. Ott, V. Panin, S. Paschalis, A. Perea, R. Plag, R. Reifarth, A. Richter, C. Rodriguez-Tajes, D. Rossi, K. Riisager, D. Savran, G. Schrieder, H. Simon, J. Stroth, K. Sümmerer, O. Tengblad, H. Weick, C. Wimmer, M.V. Zhukov, Phys. Rev. Lett. 112 (2014) 132502.
[16] V. Panin, J. Taylor, S. Paschalis, F. Wamers, Y. Aksyutina, H. Alvarez-Pol, T. Aumann, C. Bertulani, K. Boretzky, C. Caesar, M. Chartier, L. Chulkov, D. Cortina-Gil, J. Enders, O. Ershova, H. Geissel, R. Gernhäuser, M. Heil, H. Johansson, B. Jonson, A. Kelić-Heil, C. Langer, T. Le Bleis, R. Lemmon, T. Nilsson, M. Petri, R. Plag, R. Reifarth, D. Rossi, H. Scheit, H. Simon, H. Weick, C. Wimmer, Phys. Lett. B 753 (2016) 204.
[17] V. Panin, T. Aumann, C.A. Bertulani, Eur. Phys. J. A 57 (2021) 103.
[18] F. Wamers, J. Marganiec, F. Aksouh, Y. Aksyutina, H. Alvarez-Pol, T. Aumann, S. Beceiro-Novo, C.A. Bertulani, K. Boretzky, M.J.G. Borge, M. Chartier, A. Chatillon, L.V. Chulkov, D. Cortina-Gil, H. Emling, O. Ershova, L.M. Fraile, H.O.U. Fynbo, D. Galaviz, H. Geissel, M. Heil, D.H.H. Hoffmann, J. Hoffman, H.T. Johansson, B. Jonson, C. Karagiannis, O.A. Kiselev, J.V. Kratz, R. Kulessa, N. Kurz, C. Langer, M. Lantz, T. Le Bleis, C. Lehr, R. Lemmon, Y.A. Litvinov, K. Mahata, C. Müntz, T. Nilsson, C. Nociforo, W. Ott, V. Panin, S. Paschalis, A. Perea, R. Plag, R. Reifarth, A. Richter, K. Riisager, C. Rodriguez-Tajes, D. Rossi, D. Savran, G. Schrieder, H. Simon, J. Stroth, K. Sümmerer, O. Tengblad, S. Typel, H. Weick, M. Wiescher, C. Wimmer, Phys. Rev. C 97 (2018) 034612.
[19] D. Tilley, H. Weller, C. Cheves, Nucl. Phys. A 564 (1993) 1.
[20] I. Stefan, F. de Oliveira Santos, O. Sorlin, T. Davinson, M. Lewitowicz, G. Dumitru, J.C. Angélique, M. Angélique, E. Berthoumieux, C. Borcea, R. Borcea, A. Buta, J.M. Daugas, F. de Grancey, M. Fadil, S. Grévy, J. Kiener, A. Lefebvre-Schuhl, M. Lenhardt, J. Mrazek, F. Negoita, D. Pantelica, M.G. Pellegriti, L. Perrot, M. Ploszajczak, O. Roig, M.G. Saint Laurent, I. Ray, M. Stanoiu, C. Stodel, V. Tatischeff, J.C. Thomas, Phys. Rev. C 90 (2014) 014307.
[21] T. Aumann, C.A. Bertulani, J. Ryckebusch, Phys. Rev. C 88 (2013) 064610.
[22] L.V. Chulkov, G. Schrieder, Z. Phys. A 359 (1997) 231.
[23] L.V. Chulkov, T. Aumann, D. Aleksandrov, L. Axelsson, T. Baumann, M.J.G. Borge, R. Collatz, J. Cub, W. Dostal, B. Eberlein, T.W. Elze, H. Emling, H. Geissel, V.Z. Goldberg, M. Golovkov, A. Grünschloss, M. Hellström, J. Holeczek, R. Holzmann, B. Jonson, A.A. Korsheninnikov, J.V. Kratz, G. Kraus, R. Kulessa, Y. Leifels, A. Leistenschneider, T. Leth, I. Mukha, G. Münzenberg, F. Nickel, T. Nilsson, G. Nyman, B. Petersen, M. Pfützner, A. Richter, K. Riisager, C. Scheidenberger, G. Schrieder, W. Schwab, H. Simon, M.H. Smedberg, M. Steiner, J. Stroth, A. Surowiec, T. Suzuki, O. Tengblad, Phys. Rev. Lett. 79 (1997) 201.
[24] J.A. Tostevin, A. Gade, Phys. Rev. C 90 (2014) 057602.
[25] T. Aumann, C. Barbieri, D. Bazin, C. Bertulani, A. Bonaccorso, W. Dickhoff, A. Gade, M. Gómez-Ramos, B. Kay, A. Moro, T. Nakamura, A. Obertelli, K. Ogata, S. Paschalis, T. Uesaka, Prog. Part. Nucl. Phys. 118 (2021) 103847.